Vector Correlations in Photodissociation Dynamics

Paul L. Houston

Department of Chemistry, Cornell University, Ithaca, New York 14850 *(Received: January 12, 1987)*

A review is presented of the use of vector correlations in the elucidation of photodissociation dynamics. Theoretical and experimental results are discussed for four correlations among the vectors $\hat{\mathbf{E}}$, the polarization direction of the photolysis light, μ, the transition dipole of the parent molecule, $\mathbf{v}$, the recoil velocity of the fragments, and $\mathbf{J}$, the rotational angular momentum vector of a particular fragment. The four correlations to be described in detail are (1) the $\hat{\mathbf{E}}$-μ-$\mathbf{v}$ correlation, which results in an anisotropy of fragment recoil vectors in the laboratory frame; (2) the $\hat{\mathbf{E}}$-μ-$\mathbf{J}$ correlation, which results in an alignment of fragment rotational vectors in the laboratory frame; (3) the $\mathbf{v}$-$\mathbf{J}$ correlation, which, although independent of the laboratory frame, can provide information on the alignment of the molecule relative to its velocity vector; and (4) the $\hat{\mathbf{E}}$-μ-($\mathbf{v}$-$\mathbf{J}$) correlation, which combines all three effects. Other vector correlations are briefly considered through their relation to these four.

I. Introduction: Vector Correlations

Vector quantities have played an increasingly important role in the elucidation of both molecular dynamics in general and photodissociative events in particular. Wigner and Witmer,[1] Bethe,[2] Mulliken,[3] and others recognized the importance of vector correlations between a molecule and its possible fragments as early as 1928; these correlations form an essential part of modern molecular spectroscopy. Correlations influencing the dynamics of dissociative processes, however, have only been recognized during the past 20 years. This article will address three main questions. What are these vector correlations in the dynamics of photodissociation? How can they be measured? And what information do they provide? Although other vector properties can also yield dynamical information (and are discussed in section VI), we will concentrate on correlations between only a few specific vectors: the transition dipole moment μ of the parent compound, which can be aligned by the polarization vector $\hat{\mathbf{E}}$ of the dissociating light, the recoil velocity $\mathbf{v}$ of the photofragments, and the rotational angular momentum $\mathbf{J}$ of a selected photofragment.

The review below will discuss in some detail the correlations between these vectors and will attempt to provide references to historically important or particularly interesting articles in the literature, but even in a field so young it is not practical to provide a comprehensive literature survey. I will attempt instead to present simple physical explanations of the observed effects, supported when possible by more detailed theory and by examples from both the literature and our own investigations.

II. $\hat{\mathbf{E}}$-μ-$\mathbf{v}$ Correlation

Herschbach and Zare first pointed out that the vector correlation between μ and $\mathbf{v}$ can lead to an anisotropic distribution of photofragments.[4] Photolysis light with a linear polarization defined in the laboratory frame will preferentially excite those parent molecules whose dipole transition moments, μ, are aligned parallel to the electric vector, $\hat{\mathbf{E}}$, of the dissociating light. In the molecular frame, the direction of fragment departure, which defines the recoil velocity vector $\mathbf{v}$, nearly always bears a fixed angular relationship to μ; for example, in a diatomic parent molecule, $\mathbf{v}$ will be either parallel or perpendicular to μ. Consequently, if μ is aligned in the laboratory frame by the dissociating light, $\mathbf{v}$ will also be aligned in the laboratory frame, provided that the dissociation takes place rapidly enough so that the alignment of μ is not lost before the moment of fragmentation. The angular correlation between $\mathbf{v}$ and μ will thus be transformed by the dissociation into an angular correlation between $\mathbf{v}$ and $\hat{\mathbf{E}}$, as summarized in Figure 1. Zare noted that the normalized angular distribution of photofragments should be given by the equation[5]

$$I(\theta) = (4\pi)^{-1}[1 + \beta P_2(\cos\theta)] \quad (1)$$

where θ is the angle between $\mathbf{v}$ and $\hat{\mathbf{E}}$, and β is a parameter that describes the degree of anisotropy ($-1 \leq \beta \leq 2$).

An important consequence of these predictions is that the observation of an anisotropic distribution can provide information concerning the alignment of the transition dipole moment μ in the molecular frame of the parent compound; i.e., the angular distribution of the fragments will determine the symmetry of the upper state if that of the lower state is known. Consider, for example, a diatomic parent compound. An anisotropy parameter of $\beta = 2$ would give $I(\theta) \sim \cos^2\theta$. This distribution, which is peaked when $\theta = 0$, indicates that the photofragments recoil predominantly along $\hat{\mathbf{E}}$, as would be expected for μ aligned parallel to the molecular axis. On the other hand, an anisotropy parameter of $\beta = -1$ would yield $I(\theta) \sim \sin^2\theta$. The fragments in this distribution recoil predominantly perpendicular to $\hat{\mathbf{E}}$, as would be expected for μ aligned perpendicular to the molecular axis. If the parent molecules are excited from a state for example with Λ (or Ω) = 0, then in the former case they dissociate from a state with Λ (or Ω) = 0 and in the latter case from a state with Λ (or Ω) = 1.

Solomon was the first to observe an anisotropic distribution of photofragment recoil velocities.[6] Linearly polarized visible light was used to photolyze bromine or iodine within a hemispheric bulb whose inside surface had been coated with a thin film of tellurium. The pressure of the parent gas was held low enough so that the mean free path of the atomic fragments was larger than the radius of the bulb. The etching rate of the tellurium film as the atoms recoiled to the surface of the bulb was observed to depend on the angle between $\mathbf{v}$ and $\hat{\mathbf{E}}$. In both cases the flux of dissociated atoms peaked perpendicular to the electric vector of the photolysis light, and the experiment was interpreted as indicative of a perpendicular transition. This "photolysis mapping" method was later used by Solomon et al. to investigate the dissociations of aliphatic carbonyl compounds[7] but seems to have been subsequently abandoned for other techniques.

A more quantitative method for measuring recoil velocity distributions was developed in 1969 almost simultaneously by Busch et al.[8] and by Diesen, Wahr, and Adler.[9] In these experiments, a linearly polarized ruby laser was used to dissociate a halogen or interhalogen molecule, while a quadrupole mass spectrometer was employed to detect the arrival time and angular distributions of atomic fragments. The principal advantage of this detection technique was that both the direction and magnitude of the recoil velocity could be determined. In the case of I_2, for example, two peaks in the arrival time distribution were observed, corresponding to the two accessible spin-orbit states of the I atom.

(1) Wigner, E. P.; Witmer, E. E. *Z. Phys.* **1928**, *51*, 859.
(2) Bethe, H. *Ann. Phys.* **1929**, *3*, 133.
(3) Mulliken, R. S. *Phys. Rev.* **1933**, *43*, 279.
(4) Zare, R. N.; Herschbach, D. R. *Proc. IEEE* **1963**, *51*, 173.
(5) Zare, R. N. *Mol. Photochem.* **1972**, *4*, 1.
(6) Solomon, J. *J. Chem. Phys.* **1967**, *47*, 889.
(7) Solomon, J.; Jonah, C.; Chandra, P.; Bersohn, R. *J. Chem. Phys.* **1971**, *55*, 1908.
(8) Busch, G. E.; Mahoney, R. T.; Morse, R. I.; Wilson, K. R. *J. Chem. Phys.* **1969**, *51*, 449, 837.
(9) Diesen, R. W.; Wahr, J. C.; Adler, S. E. *J. Chem. Phys.* **1969**, *50*, 3635.

0022-3654/87/2091-5388$01.50/0

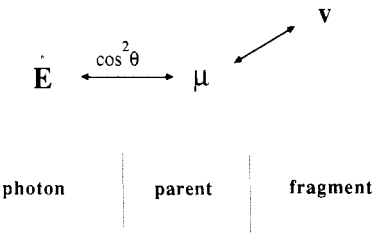

Figure 1. The μ–v correlation. Because the transition dipole of the parent, μ, and the recoil velocity of the fragment, v, are correlated in most dissociations, alignment of μ by the electric vector, $\hat{\mathbf{E}}$, of the photolysis light creates an angular correlation between $\hat{\mathbf{E}}$ and v.

An alternative technique which provides both the direction and magnitude of the recoil velocity is based on the Doppler effect. Zare and Herschbach recognized that if one fragment were produced in an excited electronic state, its emission spectrum would reveal information both about the magnitude of its velocity, as expressed in the width of the Doppler profile, and about its directional anisotropy, as expressed in the shape of the profile.[4,10] Experimental confirmation of this effect waited several years and came in a slightly different form. Schmiedl et al. monitored the Doppler profile of the (ground-state) H atom produced in the 266-nm dissociation of HI by using vacuum-UV laser-induced fluorescence.[11] For a fragment whose speed distribution is given by $F(|\mathbf{v}|) = \delta(|\mathbf{v}| - v_0)$, absorption will take place at a frequency given by $\nu = \nu_0[1 - (w/c)]$ where $w = \mathbf{v}\cdot\hat{\mathbf{k}} = v_0 \cos\chi$, called the Doppler shift, is the projection of v onto the probe direction $\hat{\mathbf{k}}$. If $\hat{\mathbf{k}}$ makes an angle θ' with respect to the electric vector of the (linearly polarized) dissociation light, then it can be shown that the Doppler profile for laser-induced fluorescence should be given by[11]

$$I(\chi) = (4\pi)^{-1}[1 + \beta P_2(\cos\theta')P_2(\cos\chi)] \qquad (2)$$

Figure 2 displays Doppler profiles observed by Schmiedl et al.[11] in the 266-nm dissociation of HI for angles $\theta' = 0°$, 45°, and 90°. For photolysis at this wavelength there are two dissociative channels, one producing H + $I(^2P_{1/2})$ via a $\Delta\Omega = 0$ (parallel) transition and another producing H + $I(^2P_{3/2})$ via a $\Delta\Omega = 1$ (perpendicular) transition. Thus, since the former channel deposits more energy into internal degrees of freedom, we expect to observe a profile composed of slower fragments recoiling with a distribution characteristic of a parallel transition ($\beta = 2$) and faster fragments recoiling with a distribution characteristic of a perpendicular transition ($\beta = -1$). Composite profiles based on eq 2 do indeed fit the data, as shown by the sum of curves a and b in Figure 2.

In the dissociation of a diatomic molecule we expect to observe at most a few product states, each corresponding to a possible internal excitation of an atomic fragment. But in the dissociation of polyatomic parent compounds, several vibrational and rotational levels of the fragment(s) might also be produced. In the case of ICN dissociation at 266 nm, for example, not only can the I atom be produced in either spin–orbit state, but the CN fragment can in principle be produced with both rotational and vibrational excitation. Experiments demonstrate that while the CN is produced predominantly in $v = 0$, its rotational distribution spans levels from $N = 0$ to almost $N = 60$. Nadler et al.[12] have have used Doppler-resolved laser-induced fluorescence not only to deconvolute the rotational distribution of the CN fragment into those components due to each of the two iodine channels but also to determine the degree of anisotropy on each rotational level for each channel. Another recent use of the Doppler technique to determine the correlation between μ and v is provided by the work by Vasudev, Zare, and Dixon on HONO.[13,14]

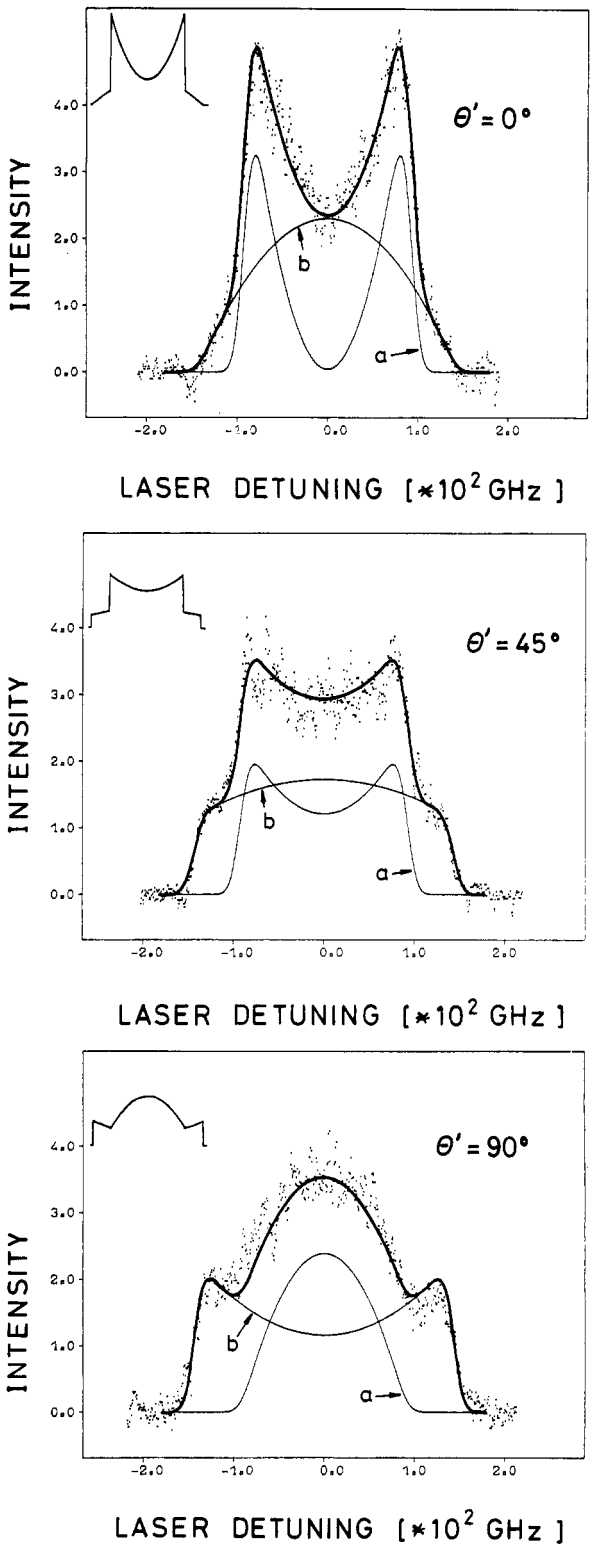

Figure 2. Experimental Doppler line profiles (dots) measured at probe angles $\theta' = 0°$, 45°, and 90°, where θ' is the angle between $\hat{\mathbf{E}}$ and $\mathbf{k}$. The theoretical profiles (a) and (b) are for pure parallel ($\beta = 2$) and perpendicular ($\beta = -1$) transitions, weighted such that superposition yields the best fits to the experimental profiles (heavy curves). Inserted in the top left corners are illustrations of the theoretical sum profiles expected under ideal resolution. Reprinted with permission from ref 11. Copyright 1982 Springer-Verlag.

In closing this section, it should be noted that the correlation between μ and v is observed by an anisotropy measured in the *laboratory* frame; observation of the correlation depends on maintenance of the alignment between $\hat{\mathbf{E}}$ and μ during the time

(10) Zare, R. N. Ph.D. Thesis, Harvard University, Cambridge, MA, 1964.
(11) Schmiedl, R.; Dugan, H.; Meier, W.; Welge, K. H. *Z. Phys. A* **1982**, *304*, 137.
(12) Nadler, I.; Mahgerefteh, D.; Reisler, H.; Wittig, C. *J. Chem. Phys.* **1985**, *82*, 3885.
(13) Vasudev, R.; Zare, R. N.; Dixon, R. N. *Chem. Phys. Lett.* **1983**, *96*, 399.
(14) Vasudev, R.; Zare, R. N.; Dixon, R. N. *J. Chem. Phys.* **1984**, *80*, 4863.

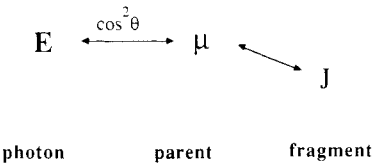

Figure 3. The μ–J correlation. Because the transition dipole of the parent, μ, and the rotational angular momentum, J, are correlated in most dissociations, alignment of μ by the electric vector, $\hat{\mathbf{E}}$, of the photolysis light creates an angular correlation between $\hat{\mathbf{E}}$ and J.

period between absorption and fragmentation. Thus, rotation of the parent compound prior to dissociation, which might be expected for example in many predissociations, will usually diminish the observed anisotropy as $\hat{\mathbf{E}}$ and μ become uncorrelated. The degree to which the anisotropy will be lost as a result of such parent rotation has been treated in detail by Jonah[15] and by Yang and Bersohn.[16] In general, the loss of anisotropy depends on the lifetime of the parent compound, its rotational temperature, and its rotational constant(s). Loss of anisotropy due to such experimental effects as the finite velocity distribution of the parent molecules, the possibility of collisions, and the finite velocity and angular resolution must also be considered, but such losses can usually be minimized by careful design of the experiment. An interesting review of results concerning recoil velocity anisotropy may be found in an article by Bersohn.[17]

III. The $\hat{\mathbf{E}}$–μ–J Correlation

A second correlation, similar to the $\hat{\mathbf{E}}$–μ–v correlation discussed above, can occur between μ, which can be aligned by $\hat{\mathbf{E}}$, and the rotational angular momentum vector of a photofragment, J. Consider, for example, the case of a triatomic parent molecule which, at the moment of dissociation, is in a bent configuration. The repulsive force between the atomic and diatomic fragments will impart a torque to the diatom, causing it to rotate about an axis perpendicular to the dissociating bond. Since this bond will have a fixed angular relationship to the transition dipole moment μ, an angular correlation will be produced between μ and J. As we have seen above, the dissociating light excites preferentially those parent compounds with μ aligned parallel to $\hat{\mathbf{E}}$. Consequently, as shown schematically in Figure 3, dissociation will also align J in the laboratory frame, provided of course that the alignment of μ is not lost due to parent rotation during the time between the excitation and dissociation steps. Van Brunt and Zare were the first to realize that such alignment of J in the laboratory by the dissociation will give rise to polarized emission in the case when the fragment is formed in an excited state.[18] If the fragment is formed in its ground state, it will absorb preferentially light of a specific polarization, as discussed by Gouedard and Lehmann,[19] Fano and Macek,[20] and Greene and Zare.[21,22]

The first experimental observation of such alignment in photodissociation was made by Chamberlain and Simons.[23,24] Dissociation of H_2O, HCN, and BrCN with linearly polarized light led to electronically excited photofragments [$OH(A^2\Sigma^+)$ and $CN(B^2\Sigma^+)$] whose emission was observed to be polarized as a result of the anisotropic distribution of J in the laboratory frame. In the classical limit for rapid dissociation of a bent triatomic molecule, the maximum degree of polarization $p \equiv (I_\parallel - I_\perp)/(I_\parallel + I_\perp)$ is given in Table I as a function of whether the absorption transition is parallel or perpendicular to the plane of the parent molecule and as a function of the orientation of the fluorescence

TABLE I: Fluorescence Polarization Limits for Dissociation of Bent Triatomics[25]

	fluorescence transition		
	parallel	perpendicular	
absorption	P, R	Q	P, R
parallel to molecular plane	$^1/_7$	$-^1/_3$	$^1/_7$
perpendicular to molecular plane	$-^1/_3$	$^1/_2$	$-^1/_3$

transition moment relative to J and to the internuclear axis.[24,25]

As in the case of $\hat{\mathbf{E}}$–μ–v correlations, $\hat{\mathbf{E}}$–μ–J correlations can be extremely useful in assigning the symmetry and lifetime of the dissociating level in the parent molecule. For example, in the case of the H_2O dissociation near 130 nm, the results of Chamberlain and Simons[23,26] showed that the polarization was negative, so that the transition dipole for the water molecule must lie in the plane of the molecule. (See Table I; with unresolved P, Q, R, emission on a perpendicular OH transition $p > 0$ if the transition dipole lies out of the molecular plane and $p < 0$ if it lies in the plane.) As a consequence, the upper state of the water molecule dissociating to produce rotationally excited OH is $^1A_1$. The technique of polarized photofluorescence excitation spectroscopy has been used extensively[27-36] and is reviewed in a recent article by Simons.[37]

When the fragments are not produced in electronically excited states, it is still possible to detect their alignment in the laboratory frame by the use of techniques such as laser-induced fluorescence (LIF).[19-22] Greene and Zare have provided a particularly compact equation for calculating the expected variation in LIF intensity as the polarization of the probe laser is varied relative to that of the dissociation source:[21]

$$I = CS \sum_{k_a,k_d,k} A_0^{(k)} \epsilon(k_d,k_a,k,0;\Omega)\ \omega(k_d,k_a,k;J_i,J_e,J_f) \quad (3)$$

In this equation, C is a constant proportional to the total population of the initial state i in the fragment; S is the product of the line strengths for the two transitions i → e and e → f in the laser-induced fluorescence; J_i, J_e, and J_f are the rotational quantum numbers of the initial, excited, and final levels, respectively; the indexes k_a and k_d refer to the multipole moments associated with the absorbed and detected photons; and k refers to the multipole moment of the overall resonance fluorescence process. For a photofragment produced by a dipole transition in the parent and for electric dipole transitions in the fragment, $k_a = 0, 2$, $k_d = 0, 2$, and $k = 0, 2$. The $A_0^{(k)}$ are the mean values of the monopole and quadrupole combinations of the angular momentum operator J. Specifically, $A_0^{(0)} = 1$ and $A_0^{(2)}$ is the expectation value of a Legendre polynomial: $A_0^{(2)} = 2\langle P_2(\hat{\mathbf{J}}\cdot\hat{\mathbf{z}})\rangle$, where $\hat{\mathbf{J}}$ is the angular momentum vector of the fragment and $\hat{\mathbf{z}}$ is a unit vector along the z axis. The function ω is given in eq 8–12 of Greene and Zare, while the function ϵ for all possible geometries is given in the appendix of the same reference. Some recent examples of LIF probing of the alignment of photofragments include studies of the dissociation of H_2O,[38,39] HONO,[13,14] ICN,[40] CH_3ONO,[41] (C-

(15) Jonah, C. *J. Chem. Phys.* **1971**, *55*, 1915.
(16) Yang, S.; Bersohn, R. *J. Chem. Phys.* **1974**, *61*, 4400.
(17) Bersohn, R. *IEEE J. Quantum Electron.* **1980**, *QE-16*, 1208.
(18) Van Brunt, R. J.; Zare, R. N. *J. Chem. Phys.* **1968**, *48*, 4304.
(19) Gouedard, G.; Lehmann, J. C. *J. Phys.* **1973**, *34*, 693.
(20) Fano, U.; Macek, J. H. *Rev. Mod. Phys.* **1973**, *45*, 553.
(21) Greene, C. H.; Zare, R. N. *J. Chem. Phys.* **1983**, *78*, 6741.
(22) Greene, C. H.; Zare, R. N. *Annu. Rev. Phys. Chem.* **1982**, *33*, 119.
(23) Chamberlain, G. A.; Simons, J. P. *Chem. Phys. Lett.* **1975**, *32*, 355.
(24) Chamberlain, G. A.; Simons, J. P. *J. Chem. Soc., Faraday Trans. 2* **1975**, *71*, 2043.
(25) Macpherson, M. T.; Simons, J. P.; Zare, R. N. *Mol. Phys.* **1979**, *38*, 2049.
(26) Macpherson, M. T.; Simons, J. P. *Chem. Phys. Lett.* **1977**, *51*, 261.
(27) Macpherson, M. T.; Simons, J. P. *J. Chem. Soc., Faraday Trans. 2* **1978**, *74*, 1965.
(28) Macpherson, M. T.; Simons, J. P. *J. Chem. Soc., Faraday Trans. 2* **1979**, *75*, 1572.
(29) Ashfold, M. N. R.; Georgiou, A. S.; Quinton, A. M.; Simons, J. P. *J. Chem. Soc., Faraday Trans. 2* **1981**, *77*, 259.
(30) Quinton, A. M.; Simons, J. P. *Chem. Phys. Lett.* **1981**, *81*, 214.
(31) Ashfold, M. N. R.; Georgiou, A. S.; Quinton, A. M.; Simons, J. P. *Nuovo Cimento Soc. Ital. Fis., B* **1981**, *63*, 21.
(32) Simons, J. P.; Smith, A. J. *Chem. Phys. Lett.* **1983**, *97*, 1.
(33) Hodgson, A.; Simons, J. P.; Ashfold, M. N. R.; Bayley, J. M.; Dixon, R. N. *Chem. Phys. Lett.* **1986**, *107*, 1.
(34) Simons, J. P.; Smith, A. J.; Dixon, R. N. *J. Chem. Soc., Faraday Trans. 2* **1984**, *80*, 1489.
(35) Hodgson, A.; Simons, J. P.; Ashfold, M. N. R.; Bayley, J. M.; Dixon, R. N. *Mol. Phys.* **1985**, *54*, 351.
(36) Hodgson, A.; Simons, J. P.; Smith, A. J.; Dixon, R. N. In *Photophysics and Photochemistry above 6eV*; Lahmani, F., Ed.; Elsevier: Amsterdam, 1985; p 505.
(37) Simons, J. P. *J. Phys. Chem.* **1984**, *88*, 1287.

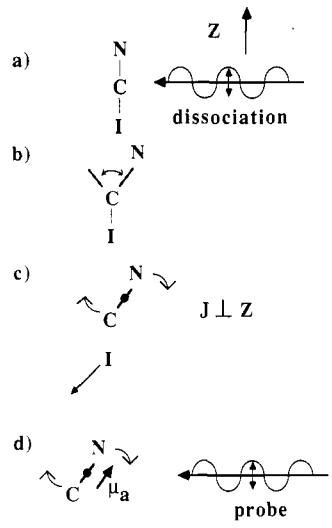

Figure 4. Rotational alignment in the photodissociation of ICN. (a) Linearly polarized photolysis light preferentially exites those ICN molecules whose transition dipole moment, assumed to lie along the ICN axis, is aligned parallel to the electric vector, taken as the Z axis. (b) The molecule bends as it dissociates, giving rise to a rotationally excited CN fragment (c) whose **J** vector is preferentially aligned perpendicular to the Z axis. (d) The CN fragment is probed by laser-induced fluorescence on a parallel transition with Z-polarized light. A strong signal is observed because rotation about **J** often aligns the absorption dipole with Z. A much weaker signal would be observed for X-polarized light since the CN absorption dipole would be aligned along X much more rarely.

$H_3)_3CONO$,[42] and $(CH_3)_2NNO$.[43]

A qualitative picture of the physical basis behind the LIF technique for measuring alignment is given in Figure 4, where the steps in the photodissociation of ICN to produce iodine atoms and rotationally excited CN are considered. Suppose that the photolysis light is linearly polarized along the Z axis as shown, and suppose also for simplicity that the ICN transition moment lies along the linear ICN axis. Because the absorption probability goes as $(\mu \cdot \mathbf{E})^2$, the excitation source will preferentially excite those molecules whose axis lies in the Z direction (Figure 4a). If the ICN molecule starts to bend as it dissociates (Figure 4b), a rotationally excited CN fragment will be produced (Figure 4c) whose angular momentum vector will be preferentially aligned perpendicular to the Z axis. (Although the **J** vector is drawn pointing out of the plane of the diagram in Figure 4, there is cylindrical symmetry about the $Z = \hat{E}$ axis.) Now suppose that the CN fragment is probed by LIF using linearly polarized light on a parallel transition (such as the $B^2\Sigma \rightarrow X^2\Sigma$ transition). Because the dipole moment for absorption of the probe laser lies parallel to the CN axis and the CN fragment is rotating about an axis, **J**, aligned preferentially perpendicular to Z, the absorption transition moment will be aligned parallel to the Z axis on nearly every rotation of the CN fragment. Since absorption of Z-polarized probe light is at a maximum when the absorption dipole is parallel to Z, a substantial signal will be seen for probe laser light polarized along the Z axis (and parallel to the polarization vector of the dissociating light). On the other hand, since **J** is preferentially perpendicular to Z, the CN fragment will seldom have its internuclear axis (and absorption moment) aligned along the X axis of Figure 4; the LIF signal corresponding to absorption of X-polarized light will be weak. This simple argument suggests that a larger signal should be observed when the pump and probe sources have their polarization vectors parellel than when they are perpendicular. Figure 5 displays the experimental results.[40] A larger signal is indeed observed when the $\hat{E}$ vectors of the two lasers are parallel. Use of eq 3 allows one to determine the alignment parameter from such data.

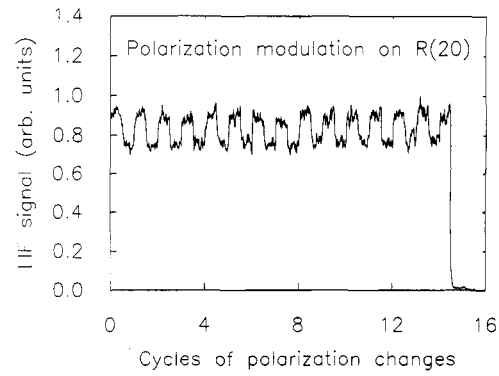

Figure 5. Intensity of laser-induced fluorescence of CN on the R(20) line following dissociation of ICN at 290 nm as the polarization of the dissociation laser is square wave modulated. The larger signals are obtained for parallel alignment of the dissociation and probe polarizations. Reprinted with permission from ref 40. Copyright 1986 American Institute of Physics.

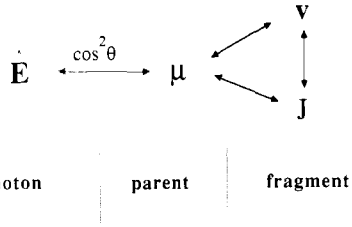

Figure 6. The v–J correlation. The transition dipole of the parent, μ, is correlated both with **v** and with **J**. Consequently, **v**, **J** are correlated even in the absence of any correlation between $\hat{E}$ and **v** or between $\hat{E}$ and **J**.

Loss of rotational alignment, like the loss of recoil velocity anisotropy discussed in the previous section, is caused by any effect that either destroys the laboratory alignment of μ prior to dissociation or scrambles the alignment of **J** prior to measurement by the probe laser. Effects in the former category include molecular rotation during the finite lifetime of the parent compound, discussed in detail by Nagata et al.,[44] while effects in the latter category include the influence of magnetic or electric fields, collisions, and depolarization due to electron and nuclear spin. This last effect has been considered in detail,[19,39,45] and formulas for correcting measured alignments are available.

IV. The v–J Correlation

Since we have seen above both that μ and **v** are correlated and that μ and **J** are correlated, it should come as not surprise that **v** and **J** are also correlated. An extremely important difference between the v–J correlation and the recoil velocity anisotropy or the rotational alignment, however, is that while the latter two effects involve correlations in the laboratory frame (mediated by the laboratory alignment of μ), the v–J correlation is completely independent of the laboratory frame. Consider again the dissociation of a bent triatomic molecule, and neglect for the moment rotation of the parent compound. Because the forces producing fragmentation operate in the plane of the parent molecule, the relative velocity **v** will also lie in that plane. The torque resulting in fragment rotation is given by $\mathbf{F} \times \mathbf{v}$, so that the rotation vector **J**, which is parallel to the torque, will lie perpendicular to the plane, and hence perpendicular to **v**. Thus, for a triatomic in the limit when **J** is much larger than the rotation of the parent, we expect to find an angular correlation between **v** and **J**: the two vectors

(38) Andresen, P.; Rothe, E. W. *J. Chem. Phys.* **1983**, *78*, 989.
(39) Andresen, P.; Ondrey, G. S.; Titze, B.; Rothe, E. *J. Chem. Phys.* **1984**, *80*, 2548.
(40) Hall, G. E.; Sivakumar, N.; Houston, P. L. *J. Chem. Phys.* **1986**, *84*, 2120.
(41) Benoist, d'Azy, O.; Lahmani, F.; Lardeux, C.; Solgadi, D. *Chem. Phys.* **1985**, *94*, 247.
(42) Schwartz-Lavi, D.; Bar, I.; Rosenwaks, S. *Chem. Phys. Lett.* **1986**, *128*, 123.
(43) Lavi, R.; Bar, I.; Rosenwaks, S. *J. Chem. Phys.*, to be published.
(44) Nagata, T.; Kondow, T.; Kuchitsu, K.; Loge, G. W.; Zare, R. N. *Mol. Phys.* **1983**, *50*, 49.
(45) Guest, J. A.; O'Halloran, M. A.; Zare, R. N. *Chem. Phys. Lett.* **1984**, *103*, 261.

TABLE II: Doppler Profiles for Isotropic Velocities and Absorption of X-Polarized Light[a,b]

case	Z	X	Y
$\mathbf{v}\|\|\mathbf{J}$, $\mathbf{J}\|\|\mu_a$	$(1/2)(\cos^2\chi - \cos^4\chi)$	$(3/8)(1 - \cos^2\chi)^2$	$(1/8)(1 - \cos^2\chi)^2$
$\mathbf{v}\|\|\mathbf{J}$, $\mathbf{J}\perp\mu_a$	$(1/8)(1 - \cos^4\chi)$	$(1/32)(3 + 2\cos^2\chi + 3\cos^4\chi)$	$(1/32)(1 + 6\cos^2\chi + \cos^4\chi)$
$\mathbf{v}\perp\mathbf{J}$, $\mathbf{J}\|\|\mu_a$	$(1/16)(1 + 2\cos^2\chi - 3\cos^4\chi)$	$(1/64)(9 + 6\cos^2\chi + 9\cos^4\chi)$	$(1/64)(3 + 2\cos^2\chi + 3\cos^4\chi)$
$\mathbf{v}\perp\mathbf{J}$, $\mathbf{J}\perp\mu_a$	$(1/64)(5 + 6\cos^2\chi - 3\cos^4\chi)$	$(1/256)(41 - 26\cos^2\chi + 9\cos^4\chi)$	$(1/256)(35 - 30\cos^2\chi + 3\cos^4\chi)$

[a] With emission polarized along the axis indicated. For absorption of Y-polarized light, the entries for the X and Y columns should be reversed. [b] Reference 53.

should be perpendicular. Note, however, that the correlation between $\mathbf{v}$ and $\mathbf{J}$ is not made until the instant of dissociation. As shown schematically in Figure 6, the $\mathbf{v}$–$\mathbf{J}$ correlation does not depend on the dissociation lifetime relative to rotation of the parent compound. It will persist even for predissociating parent molecules with long lifetimes. Of course, if all dissociations required $\mathbf{v}$ to be perpendicular to $\mathbf{J}$, as for triatomics, this correlation would not be very interesting. However, for parent molecules of four atoms or larger, and indeed even for triatomics which are rotating before absorption, there is no strict requirement on the correlation between $\mathbf{v}$ and $\mathbf{J}$; it represents a new observable that can provide detailed information about the dissociation process.

But how do we observe the $\mathbf{v}$–$\mathbf{J}$ correlation? Case, McClelland, and Herschbach,[46] in considering angular momentum polarization in molecular collisions, suggested as early as 1978 that alignment of $\mathbf{J}$ might cause difficulties in using the newly developed Doppler method[47] for measurement of velocity distributions in crossed molecular beam experiments. However, several years passed before the exact effect of $\mathbf{v}$–$\mathbf{J}$ correlation on the Doppler profile was calculated and before experimental results on molecular photodissociation became available. It is interesting to note that observation of $\mathbf{v}$–$\mathbf{J}$ correlation was made nearly simultaneously and independently in four laboratories[48-51] and that three independent explanations were put forth.[48,49,52] Before discussing the theory and results in detail, let us first consider the basic physics of the effect.

Measurement of the $\mathbf{v}$–$\mathbf{J}$ correlation is based on interpretation of the Doppler profile, as measured using polarized light. The basic physics behind the measurement can be illustrated most easily by considering the Doppler absorption profile of a photofragment whose $\mathbf{J}$ vector is constrained by the dissociation mechanism to lie parallel to its recoil velocity $\mathbf{v}$. This constraint, which is the opposite of that expectred for a triatomic parent molecule, might occur, for example, in an $(AB)_2 \rightarrow AB + AB$ fragmentation if dissociation were accompanied by substantial torsion about an axis parellel to the recoil. To emphasize the effect, we will assume that there is no correlation either between $\mathbf{J}$ and $\hat{\mathbf{E}}$ or, in particular, between $\mathbf{v}$ and $\hat{\mathbf{E}}$, so that in the absence of $\mathbf{v}$–$\mathbf{J}$ correlation the absorption as a function of Doppler shift should be constant for shifts within the allowed velocity range (eq 2 with $\beta = 0$). Imagine that the fragment is probed by absorption of light propagating along the Z ($\equiv\hat{k}$) axis and linearly polarized with $\hat{\mathbf{E}}$ along the X axis. As shown in Figure 7, fragments absorbing in the wings of the Doppler profile, i.e., those moving parallel to the probe direction $\hat{k}$, will have $\mathbf{J}\|\mathbf{Z}$, while those absorbing in the center of the Doppler profile, i.e., those moving perpendicular to $\hat{k}$, will have $\mathbf{J}\perp\mathbf{Z}$. If the fragment is probed on a Q-branch transition, for which the transition dipole of the fragment, μ_a, is parallel to $\mathbf{J}$ in the classical limit, we find that $\mu_a\|\mathbf{Z}$ ($\mu_a\perp\hat{\mathbf{E}}$) in the wings and $\mu_a\perp\mathbf{Z}$ (μ_a in the X–Y plane) in the center of the Doppler profile. Since the absorption is proportional to $|\mu_a\cdot\hat{\mathbf{E}}|^2$, there will be no absorption in the wings and substantial absorption in the center. If, on the other hand, the same fragment were probed by using a P- or R-branch transition, for which $\mu_a\perp\mathbf{J}$, it can easily be shown by similar arguments that there would be absorption both in the wings and in the center of the profile, with more absorption in the wings. Thus, fragments with $\mathbf{v}\|\mathbf{J}$ will present different absorption profiles depending on whether they are probed with Q-branch or P-, R-branch transitions. If $\mathbf{v}$ were completely uncorrelated with $\mathbf{J}$, there would be no difference in Doppler profiles measured with different transitions; absorption at all Doppler shifts within the allowed velocity range would be of the same intensity.

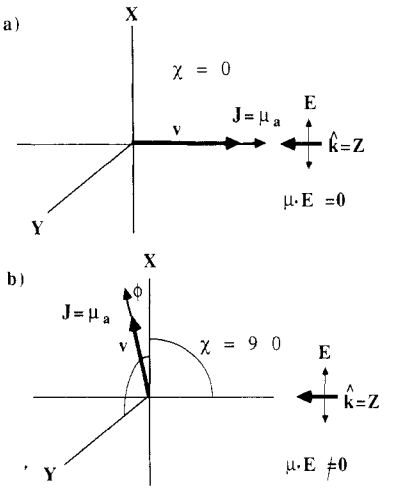

Figure 7. The Doppler profile when $\mathbf{v}$ and $\mathbf{J}$ are correlated parallel to one another and when probed on a Q-branch line of a perpendicular transition (for which μ_a is parallel to $\mathbf{J}$): (a) fragments absorbing in the wings of the Doppler profile will have $\mu_a\|Z$, while (b) those absorbing in the center of the Doppler profile will have μ_a in the X–Y plane. If $\hat{\mathbf{E}}$ is along X, since the absorption is proportional to $|\mu_a\cdot\hat{\mathbf{E}}|^2$, there will be no absorption in the wings and substantial absorption in the center.

The above example has been chosen to demonstrate how the manifestation of $\mathbf{v}$–$\mathbf{J}$ correlation in the Doppler absorption profile can be determined by simple physics. It has been overly specific in that it considered only $\mathbf{v}\|\mathbf{J}$, only isotropic recoil velocities, and only absorption. Much more general treatments have been presented elsewhere[48,52,53] which consider differing degrees of $\mathbf{v}$–$\mathbf{J}$ correlation and probing by laser-induced fluorescence, where both absorption and emission steps must be included. The general result for isotropic velocity distributions is that the Doppler profile is given by an even polynomial in cox χ of order 4. In the limiting cases of $\mathbf{v}$ parallel or perpendicular to $\mathbf{J}$, these polynomials for LIF probe light propagating along Z and polarized along X are given in Table II,[52,53] where linearly polarized fluorescence is detected along the axis listed at the head of the columns. For detection of unpolarized fluorescence, the results of two columns must be added; e.g., unpolarized fluorescence propagating along the Y axis would have an LIF signal given by the sum of corresponding entries in the Z and X columns.

An example of the usefulness of the $\mathbf{v}$–$\mathbf{J}$ correlation is provided by the dissociation of glyoxal.[54] When excited to low-lying

(46) Case, D. A.; McClelland, G. M.; Herschbach, D. R. *Mol. Phys.* **1978**, *35*, 541.
(47) Kinsey, J. L. *J. Chem. Phys.* **1977**, *66*, 2560.
(48) Hall, G. E.; Sivakumar, N.; Houston, P. L.; Burak, I. *Phys. Rev. Lett.* **1986**, *56*, 1671.
(49) Dubs, M.; Brühlmann, U.; Huber, J. R. *J. Chem. Phys.* **1986**, *84*, 3106.
(50) Gericke, K.-H.; Klee, S.; Comes, F. J.; Dixon, R. N. *J. Chem. Phys.* **1986**, *85*, 4463.
(51) Docker, M. P.; Hodgson, A.; Simons, J. P. *Chem. Phys. Lett.* **1986**, *128*, 264; *Faraday Discuss. Chem. Soc.*, in press.
(52) Dixon, R. N. *J. Chem. Phys.* **1986**, *85*, 1866.
(53) Hall, G. E.; Sivakumar, N.; Chawla, G.; Houston, P. L.; Burak, I., submitted for publication.
(54) Burak, I.; Hepburn, J. W.; Sivakumar, N.; Hall, G. E.; Chawla, G.; Houston, P. L. *J. Chem. Phys.* **1987**, *86*, 1258.

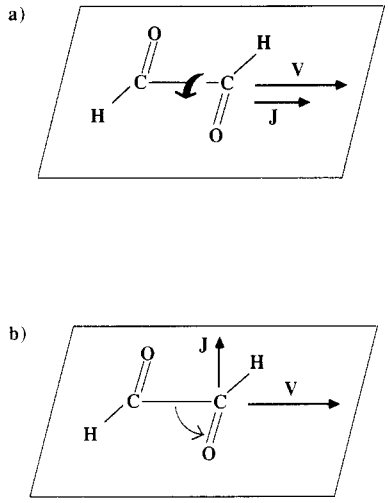

Figure 8. Two models for the dissociation of glyoxal (CHOCHO). In (a) the dissociation is accompanied by substantial torsional motion about the C–C bond, resulting in rotation of the CO product such that J and v are parallel. In (b) the dissociation takes place entirely in the original plane of the glyoxal, so that CO rotation is in this plane and J and v are perpendicular.

vibrational levels of S_1, glyoxal, which is trans-planar in the ground state, dissociates to give CO and a variety of partners:

$$\mathrm{CHOCHO} + h\nu \rightarrow \mathrm{H_2CO} + \mathrm{CO} \quad (4)$$

$$\rightarrow \mathrm{H_2} + 2\ \mathrm{CO} \quad (5)$$

$$\rightarrow \mathrm{HCOH} + \mathrm{CO} \quad (6)$$

Because the dissociation is predissociative with lifetimes on the order of 1 μs, it is expected that parent rotation will largely destroy any correlations of J or v with $\hat{\mathbf{E}}$. If the CO fragments had a single speed, the isotropic velocity distribution would be expected, in the absence of v–J correlation, to result in an LIF signal which is constant as a function of Doppler shift within the limits of $\nu_0(1 \pm v_0/c)$.

Before considering the Doppler profiles expected if there is a v–J correlation, let us first consider what dynamical constraints might give rise to a correlation. Figure 8 depicts two limiting cases of glyoxal dissociation which produce rotationally excited CO. In the first case, the glyoxal dissociation is accompanied by substantial torsional motion about the C–C axis. If this torsion were the principal source of the CO rotation, then we would expect J and v to be parallel, as shown in Figure 8a. On the other hand, if dissociation were to take place completely in the plane of the original glyoxal molecule, we would expect J and v to be perpendicular, as shown in Figure 8b. [In the latter case, even though J will be expected to have a particular (perpendicular) alignment with respect to the molecular plane, parent rotation, which is expected to destroy the anisotropy, will also ensure that J is nearly axially symmetric about v.] We have seen from Figure 7 that when J and v are parallel, we expect Q lines to absorb in the center of the Doppler profile but not in the wings. Nearly the converse will be true for P and R lines when J and v are parallel; LIF on these lines will show signal in the wings but have a substantial dip in the center of the profile. By contrast, when J and v are perpendicular, it is the Q lines which show a dip in the center and P and R lines which show reduced signal in the wings.

The actual profiles expected for the geometry employed,[54] for a single CO speed, and for the assumption that J is perpendicular to v are shown in row e of Figure 9. Of course, with three possible dissociation channels and with differing internal energies in the sibling fragments, the CO will have a wide distribution of speeds. Row d of Figure 9 gives the Doppler profiles expected if the CO speed distribution is Boltzmann with $T = 5600$ K. Note that the dip in the center of the Q lines persists. Rows a–c show data for three representative J values. The distinctive line shapes of the Q vs. P, R lines persist throughout the complete Doppler profile data set spanning $J'' = 20$–59. In all cases the Q lines exhibit

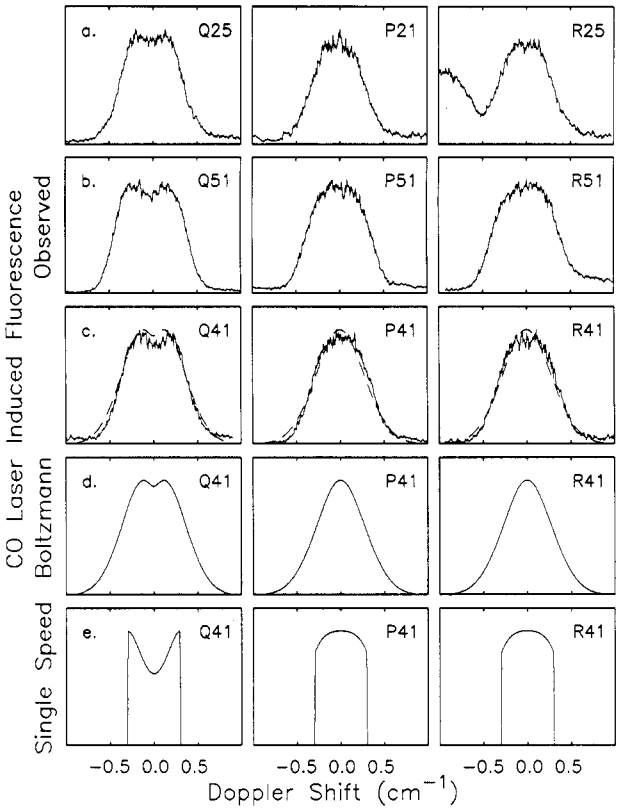

Figure 9. Calculated and experimental profiles for CO produced in the photodissociation of glyoxal. Rows a–c: representative experimental data for Q(J'') (left), P(J'') (center), and R(J'') (right) transitions. The distinctive line shapes of the Q vs. P. R. lines persist throughout the complete Doppler profile data set spanning $J'' = 20$–59. Rows d and e: calculated Doppler profiles assuming a $\mathbf{v} \perp \mathbf{J}$ correlation. Row e is for a single CO recoil velocity, while row d is for a Boltzmann distribution of recoil speeds. The dashed line in row c is a superposition onto the data of the Doppler profile shown in row d. Reprinted with permission from ref 54. Copyright 1987 American Institute of Physics.

a dip in the center of the profile, whereas the P and R lines do not. The observations are thus in accord with the planar dissociation depicted in Figure 8b, which is also the transition state predicted from ab initio calculations.[55]

Although the v–J correlation is most noticeable when the fragment is probed by using a perpendicular transition where Q lines can be compared to P and R lines, the correlation is manifest, though less obvious, even for parallel transitions in the fragment. In general, the shapes of any of the lines will be different from those expected in the absence of v–J correlation (due especially to the quartic term, Table II), and the Doppler profile will change with the angle and polarization of fluorescence detection. An example of this last effect is shown in Figure 10, where LIF Doppler profiles for unpolarized fluorescence detected along three axes are shown for the case of isotropic velocities and a probe laser propagating along Z, polarized along X, and exciting a parallel transition in the fragment.

The glyoxal example cited above makes clear two of the main features of the v–J correlation: (1) the correlation can provide information about the transition state in the dissociation, and (2) the correlation persists even when the correlation between μ and $\hat{\mathbf{E}}$ (and hence those between v and $\hat{\mathbf{E}}$ and between J and $\hat{\mathbf{E}}$) are destroyed.

V. The $\hat{\mathbf{E}}$–μ–(v–J) Correlation

We now consider the case for which, in addition to the v–J correlation, μ is also correlated with $\hat{\mathbf{E}}$. In this case, it is reasonable to expect that the Doppler profile will be affected both by the v–J correlation and by the laboratory-defined anisotropy of recoil

(55) Osamura, Y.; Schaefer, H. F.; Dupuis, M.; Lester, W. A. *J. Chem. Phys.* **1981**, *75*, 5828.

TABLE III: $G(\cos\chi)$ for Absorption of X-Polarized Light[a,b]

case	Z	X	Y
$v\|\|J, J\|\|\mu$	$(9/16)(\cos^2\chi - \cos^4\chi)$	$(15/32)(1 - \cos^2\chi)^2$	$(3/32)(1 - \cos^2\chi)^2$
$v\|\|J, J\perp\mu$	$(3/64)(1 + 2\cos^2\chi - 3\cos^4\chi)$	$(3/128)(1 + 2\cos^2\chi + 5\cos^4\chi)$	$(3/128)(1 + 6\cos^2\chi + \cos^4\chi)$
$v\perp J, J\|\|\mu$	$(3/128)(1 + 8\cos^2\chi - 9\cos^4\chi)$	$(9/256)(1 + 2\cos^2\chi + 5\cos^4\chi)$	$(3/256)(3 + 2\cos^2\chi + 3\cos^4\chi)$
$v\perp J, J\perp\mu$	$(3/512)(13 + 12\cos^2\chi - 9\cos^4\chi)$	$(3/1024)(51 - 42\cos^2\chi + 15\cos^4\chi)$	$(3/1024)(35 - 30\cos^2\chi + 3\cos^4\chi)$

[a] With emission polarized along the axis indicated. [b] Reference 53.

TABLE IV: $G(\cos\chi)$ for Absorption of Y-Polarized Light[a,b]

case	Z	X	Y
$v\|\|J, J\|\|\mu$	$(3/16)(\cos^2\chi - \cos^4\chi)$	$(3/32)(1 - \cos^2\chi)^2$	$(3/32)(1 - \cos^2\chi)^2$
$v\|\|J, J\perp\mu$	$(3/64)(3 - 2\cos^2\chi - \cos^4\chi)$	$(3/128)(1 + 6\cos^2\chi + \cos^4\chi)$	$(3/128)(5 + 2\cos^2\chi + \cos^4\chi)$
$v\perp J, J\|\|\mu$	$(9/128)(1 - \cos^4\chi)$	$(3/256)(3 + 2\cos^2\chi + 3\cos^4\chi)$	$(9/256)(5 + 2\cos^2\chi + \cos^4\chi)$
$v\perp J, J\perp\mu$	$(3/512)(7 + 12\cos^2\chi - 3\cos^4\chi)$	$(3/1024)(35 - 30\cos^2\chi + 3\cos^4\chi)$	$(3/1024)(31 - 10\cos^2\chi + 3\cos^4\chi)$

[a] With emission polarized along the axis indicated. [b] Reference 53.

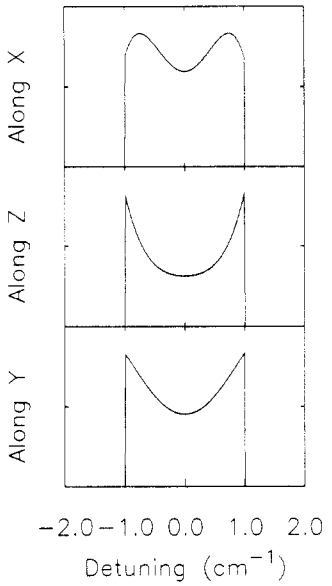

Figure 10. Doppler profiles as a function of fluorescence detection geometry. It is assumed that, although the velocity distribution is isotropic, a perpendicular correlation is maintained between v and J. The fragment is probed on the P or R line of a parallel transition with light which propagates along Z and is polarized along X. Unpolarized fluorescence detection is along the axes shown. Note that the Doppler profile changes substantially with detection geometry.

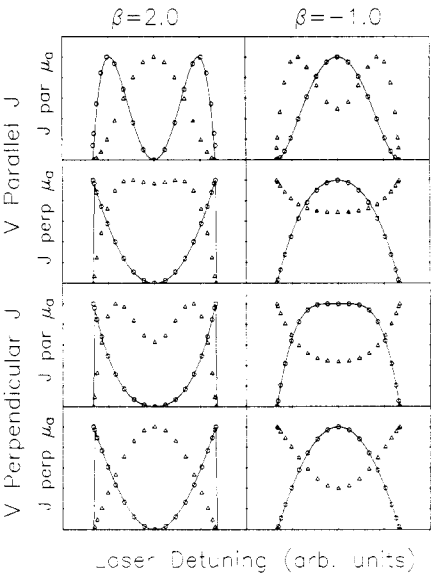

Figure 11. Doppler profiles for the limiting cases of v parallel or perpendicular to J. The parameter β describes the anisotropy of recoil velocities. Solid and dotted lines are the prediction of the classical theory, while the triangles and circles are the prediction of the quantum theory. Solid lines and circles are for $\hat{E}$ along the propagation direction of the probe laser, while dotted lines and triangles are for $\hat{E}$ perpendicular to that direction. "J par μ_a" and "J perp μ_a" refer to the orientation of the fragments rotation with respect to its transition dipole. The former should be used for Q-branch transitions, and the latter for P- and R-branch transitions. Reprinted with permission from ref 53. Copyright American Institute of Physics.

velocities. In the limiting cases of v parallel or perpendicular to J, it is possible to predict the Doppler profile using classical mechanics, but in the more general case, when v and J are not so strongly correlated, it is most practical to use a quantum mechanical approach. Since the limiting cases provide very simple formulas whereas the general case is much more complicated, the classical and quantum approaches will be summarized separately.

A. Classical Mechanical Description. A classical description of the $\hat{E}$–μ–(v–J) correlation has been presented as a section in a recent article by Hall et al.[53] The general approach is to consider the two limits of the v–J correlation in a diatomic fragment: v parallel to J and v perpendicular to J. In general, for each of these limits there will also be two possible alignments of the fragment transition dipole μ_a with respect to J: parallel to J, as for a Q-branch line of a perpendicular transition (in the high-J limit), or perpendicular to J, as for all lines of a parallel transition and R- and P-branch lines of a perpendicular transition. There are thus four limiting cases to consider: $v\|J, J\|\mu_a$; $v\|J, J\perp\mu_a$; $v\perp J, J\|\mu_a$; $v\perp J, J\perp\mu_a$.[56] For each of these four cases, the possible angles of μ_a with respect to the probe laser polarization vector ϵ_a and with respect to the fluorescence detection polarization vector ϵ_f are calculated. Then the absorption transition, $|\mu_a\cdot\epsilon_a|^2$, and the fluorescence transition, $|\mu_a\cdot\epsilon_f|^2$, for the fragment are each averaged over any azimuthal angles that change between absorption and emission, and their product, weighted by the number of fragments recoiling into a particular direction, is averaged over any remaining azimuthal angles. If it is assumed that J is axially symmetric about v,[57] the result is

$$D(\cos\chi) \propto \mathrm{ADF}(\cos\chi)[1 + \beta P_2(\cos\chi\cos\theta')] + \beta(1 - \cos^2\chi)\sin^2\theta' G(\cos\chi) \quad (7)$$

where $\mathrm{ADF}(\cos\chi)$ is the function listed in Table II and $G(\cos\chi)$ is a fourth-order polynomial in $\cos\chi$ listed for each of the four cases and each of the three detection polarizations in Table III for absorption of X-polarized light and in Table IV for absorption of Y-polarized light. Note that when the probe direction and the

(56) There are actually six limiting cases, since when $J\perp v$ we can have either of the two limits $J\|\mu$ or $J\perp\mu$. In the discussion which follows we will assume for simplicity that J is axially symmetric about v; the $J\|\mu$ or $J\perp\mu$ limits can be accounted for simply by including the proper weighting function in the integrand described below.

(57) We have assumed here that the fluorescence transition is of the same symmetry as the absorption transition, but this may be easily modified for more complicated LIF probing transitions. Furthermore, it is usual for J not to be axially symmetric about v due to the correlation of J with μ. In such cases the proper weighting function for the azimuthal angle of J about μ must be included before integration (see footnote 56).

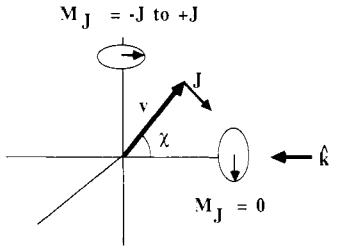

Figure 12. M_J distribution as a function of Doppler shift, cos χ, when **v** and **J** are perpendicular. Reprinted with permission from ref 53. Copyright American Institute of Physics.

polarization direction of the dissociating light are parallel, then $\theta' = 0$ and $D(\cos\chi) = \mathrm{ADF}(\cos\chi)[1 + \beta P_2(\cos\chi)]$; that is, the overall Doppler profile for the $\hat{\mathbf{D}}$–μ–(**v**–**J**) correlation is simply the product of the profiles expected for the $\hat{\mathbf{E}}$–μ–**v** and **v**–**J** correlations.

Doppler profiles for the four cases discussed above are presented in Figure 11, where it has been assumed that X-polarized light propagating along Z is absorbed by the fragments and that the detector is located on the Y axis and does not discriminate fluorescence polarizations. The figure gives the profiles (shown as lines) for either $\beta = 2$ or $\beta = -1$ and for two values of the angle between $\hat{\mathbf{E}}$ and the probe laser direction, namely, $\theta' = 0$ (solid lines) or $\theta' = \pi/2$ (dotted lines). The symbols in the figure will be discussed later. Note that the Doppler profile is a sensitive function of the anisotropy parameter β, the **v**–**J** correlation limit, and the geometry given by θ'.

B. Quantum Mechanical Description. Two quantum mechanical descriptions have recently appeared. One, presented by Hall et al.,[48,53,58] is based on a density matrix approach, while a second, presented by Dixon,[52] is based on expansion of the correlated angular momentum and velocity distribution in terms of the expectation values of bipolar harmonics. We summarize each of these approaches below.

The approach by Hall et al.[48,53,58] is best suited for calculating the Doppler profile from an assumed correlation of **v** and **J**. Consider the case when the Doppler profile is measured with light propagating along a Z axis which makes an angle θ' with respect to the electric vector of the linearly polarized dissociating light. The Doppler profile of molecules moving in a direction specified by the polar angle χ and the azimuthal angle ϕ with respect to the propagation direction will depend (1) on the number of fragments recoiling into this angle and (2) on their M_J distribution on the Z axis, taken here to be the direction of propagation. That this M_J distribution changes with χ can be seen from Figure 12, which considers the case when **v** and **J** are perpendicular.

Molecules recoiling at polar and azimuthal angles χ and ϕ with respect to the direction of propagation will make a specified polar angle, θ, with respect to the electric vector of the dissociating light. The angle θ is related to the angles θ', χ, and ϕ by the condition

$$\cos\theta = \cos\theta'\cos\chi + \sin\theta'\sin\chi\sin\phi \qquad (8)$$

where ϕ is measured from the plane containing the probe direction and the polarization vector of the dissociation laser. In order to calculate the Doppler profile, we need to ascertain the M_J distribution on the Z axis of propagation, but the correlation between **v** and **J** is most conveniently described in the molecular frame with **v** as the axis of quantization. We define the probabilities for projections M_v of **J** onto **v** to be the diagonal elements of a density matrix $\rho(\theta)$. In the special case when the vector **J** is azimuthally symmetric about **v**, all off-diagonal elements of $\rho(\theta)$ will be zero. The density matrices corresponding to the two basis sets M_v and M_J are related by a unitary transformation[59]

$$\rho'(\chi,\theta',\phi) = [D(-\phi,\chi,\phi)]^{-1}\,\rho(\theta)[D(-\phi,\chi,\phi)] \qquad (9)$$

where $\rho(\theta)$ describes the distribution of projections of **J** onto **v** and $\rho'(\chi,\theta',\phi)$ contains diagonal elements, describing the probabilities for projections of **J** onto Z, and off-diagonal elements, describing the coherences. The intensity of laser-induced fluorescence for molecules described by the matrix ρ' is given by[60-62]

$$I(\chi,\theta') \sim \int \mathrm{d}\phi\; W(\chi,\theta',\phi)\;\mathrm{Tr}\;\mathbf{A}\cdot\mathbf{F} \qquad (10)$$

where $W(\chi,\theta',\phi) = 1 + \beta P_2(\cos\theta)$ gives the probability of recoil into a given direction and matrices **A** and **F** describe the absorption and fluorescence steps, respectively. The matrices **A** and **F** are given by

$$A_{MM'} = \sum\langle J'K'M|\Phi|JKM_J'\rangle\rho'(M_J'M_J)\langle JKM_J|\Phi|J'K'M'\rangle \qquad (11)$$

$$F_{M'M} = \sum\langle J'K'M|\Phi|JKM_J\rangle\langle JKM_J|\Phi|J'K'M\rangle \qquad (12)$$

where the summation is over $M_J'M_J$ from $-J$ to J and $|JKM\rangle$ are the symmetric-top wave functions. For linear polarizations the Φ matrices occurring in the absorption or fluorescence steps can be described as a sum

$$\Phi = \sum_F\sum_g \lambda_F\lambda_g\Phi_{Fg} \qquad (13)$$

where $F = X, Y, Z$ are the laboratory coordinates, $g = x, y, z$ are the molecular coordinates, and the coefficients λ_F are the projections of the electric vector onto the laboratory coordinates, while the coefficients λ_g are the projections of the dipole moment onto the molecular coordinates. Φ_{Fg} are elements of the direction of cosine matrix, listed elsewhere.[63]

$I(\chi,\theta')$ in eq 10 gives the intensity of laser-induced fluorescence as a function of Doppler detuning, χ, for any particular relative angle θ' between the polarization vector of the dissociation laser and the probing direction. For the limiting cases of **v** perpendicular or parallel to **J**, calculations using this equation for the parameters listed in the caption to Figure 11 and for $J = 20$ give the circles and triangles in that figure. Note that there is essentially perfect agreement between the classical and quantum descriptions, as expected for the high-J limit. It should be emphasized, however, that the theory is not restricted to these limiting cases; any degree of correlation between **v** and **J** can be described by using appropriate elements of the density matrix $\rho(\theta)$.

The quantum mechanical approach by Dixon[52] has the advantage that, in principle, one can invert an observed Doppler profile to obtain the moments of the correlated angular momentum and recoil velocity distribution. Bipolar spherical harmonics are defined by the equation

$$B_{KQ}(k_1k_2;\theta_t\phi_t\theta_r\phi_r) = \sum_{q_1}\sum_{q_2}(-1)^{K-Q}[2K+1]^{1/2}\begin{pmatrix} k_1 & K & k_2 \\ q_1 & -Q & q_2\end{pmatrix}C_{k_1q_1}(\omega_t)\,C_{k_2q_2}(\omega_r) \qquad (14)$$

where $C_{kq}(\omega_t)$ and $C_{kq}(\omega_r)$ are modified shperical harmonic functions. They span the complete set of functions in the space defined by the two directions ω_r and ω_t, so that their expectation values provide a complete description of the correlated distribution. Dixon's approach is to expand the moments of the rotational distribution, (the $A_q^{(k)}$ of eq 3) as functions of the Doppler shift by using expectation values of these bipolar harmonics. For detection by laser-induced fluorescence, the general formula for the Doppler profile is then given by an equation similar to eq 3

$$I = CS\sum_{k_a,k_d,k,q} A_q^{(k)}(J_i)\epsilon'(k_d,k_a,k,q;\Omega)\;\gamma'(k_d,k_a,k;J_i,J_e,J_f) \qquad (15)$$

where the $A_q^{(k)}$ are now functions of the Doppler shift. Substitution of the expansions for $A_q^{(k)}$ into eq 15 leads to a very cumbersome expression, but for normal geometries of pump and probe directions and polarizations, the profile in each case can be described by a function of the form

(58) Hall, G. E.; Sivakumar, N.; Ogorzalek, R.; Chawla, G.; Haerri, H.-P.; Houston, P. L.; Burak, I.; Hepburn, J. W. *Discuss. Faraday Soc.* **1986**, *82*, 13.
(59) Edmonds, A. R. *Angular Momentum in Quantum Mechanics*; Princeton University Press: Princeton, NJ, 1957; p 61.
(60) Breit, G.; Lowen, I. S. *Phys. Rev.* **1934**, *46*, 590.
(61) Franken, P. A. *Phys. Rev.* **1961**, *121*, 508.
(62) Zare, R. N. *J. Chem. Phys.* **1966**, *45*, 4510.
(63) Cross, P. C.; Hainer, R. M.; King, G. W. *J. Chem. Phys.* **1944**, *12*, 210.

$$I(\cos\chi) = g_0 + g_2P_2(\cos\chi) + g_4P_4(\cos\chi) + g_6P_6(\cos\chi) \quad (16)$$

Note that this is an even polynomial of order six in the Doppler shift, just as is eq 7.

The coefficients g_i in eq 16 have been tabulated for each of a variety of experimental geometries.[52] In general, they each depend on several of the bipolar moments of the correlated distribution. By extracting the g_i from the data and solving simultaneous equations for the bipolar moments, one can in principle invert the Doppler profile to obtain the correlated distribution. In practice, however, this inversion appears to be rather difficult, so that one must either approximate the fit to the Doppler profile to obtain the principal moments and then refine the approximations or simply assume a particular correlation and then calculate the expected Doppler profile via eq 15. In the latter case, the procedure is similar to that used by Hall et al.[48,53,58]

Either of these quantum mechanical approaches can be used to determine from the experimentally measured Doppler profiles the distribution of fragment angular momentum vectors in the laboratory frame as a function of recoil angle. For triatomic dissociations, Balint-Kurti and Shapiro[64,65] have shown how to calculate this distribution from knowledge of the potential energy surfaces controlling the dissociation and of the excited-state transition moment function. It should be possible in principle, therefore, to use information obtained from the Doppler profiles to gain knowledge of the potential energy surfaces and the transition moment function when these are unknown. This goal, yet to be achieved in practice, represents for photodissociation dynamics the strongest link obtainable between experiment and theory.

C. Experimental Examples. Three photodissociation systems demonstrating the complete $\hat{E}$–μ–(v–J) correlation have been reported to date. Hall et al.[48] investigated the photodissociation of OCS, for which it is expected on the basis of conservation of angular momentum that the J for the CO product will be perpendicular to v. If we neglect the angular momentum of $S(^1D)$ and that of the photon, both of which are much smaller than J, then conservation gives $\mathbf{J}_{OCS} = \mathbf{L} + \mathbf{J}$, where L is the orbital angular momentum. The OCS parent in these experiments was expanded in a supersonic beam, so that we expect $J_{OCS} \simeq 0$. Therefore, $\mathbf{L} \simeq -\mathbf{J}$, and since L must be perpendicular to v, we expect that $\mathbf{J} \perp \mathbf{v}$.

The experimental data for $J = 59$ are presented in Figure 13. The lower row of panels in this figure displays the experimental data (dots) and the convolution of the laser line width (0.14-cm^{-1} fwhm) with the Doppler profiles predicted by eq 10 with $\beta = 0.6$ (solid lines) assuming v and J to be perpendicular. The upper row of panels shows the convoluted profiles expected in the absence of any v–J correlation for an anisotropy parameter of $\beta = 0.6$. Along each row, the left panel is for the Q(59) line with the electric vector of the dissociating light $\hat{\mathbf{E}}$ aligned perpendicular to the propagation vector of the probe light Z ($\theta' = 90°$), the second panel is for the Q(59) line with $\hat{\mathbf{E}} \| \mathbf{Z}$ ($\theta' = 0°$), the third panel is for the P(59) line with $\hat{\mathbf{E}} \perp \mathbf{Z}$ ($\theta' = 90°$), and the last panel is for the P(59) line with $\hat{\mathbf{E}} \| \mathbf{Z}$ ($\theta' = 0°$). The laser line width is given as the dotted line in the first panel. It is clear from the figure that line shapes in the presence of v–J angular correlation (solid lines, bottom row) are qualitatively different from those when there is no correlation (solid lines, top row) and that there are differences in the line shapes depending on the transition probed and the angle θ'.

Dubs, Brühlmann, and Huber[49] investigated the photodissociation of dimethylnitrosamine [DMN, $(CH_3)_2NNO$] to produce rotationally excited NO, which was probed by two-photon laser-induced fluorescence. An appendix to their paper considers in detail the two-photon LIF of polarized molecules and provides an equation similar to eq 3 for the variation in LIF intensity with alignment. By combining Doppler profiles taken at two different angles, these authors were able to show that, in principle, it is possible to obtain both the velocity distribution and the velocity-dependent anisotropy parameter $\beta(v)$. For the dimethylnitrosamine system a value of $\beta \simeq -0.5$ was obtained when averaged over the velocity distribution. In addition, different Doppler profiles were obtained when the NO was probed on R or S transitions originating from the same rotational level. Although the signal-to-noise ratio did not allow a quantitative analysis, the data were consistent with a dissociation described by a perpendicular correlation of v with J. Since DMN has a planar C_2NNO skeleton in the ground state, it appears that the transition state in the dissociation is also planar and that the forces responsible for the recoil and for the torque on the NO group operate in the plane.

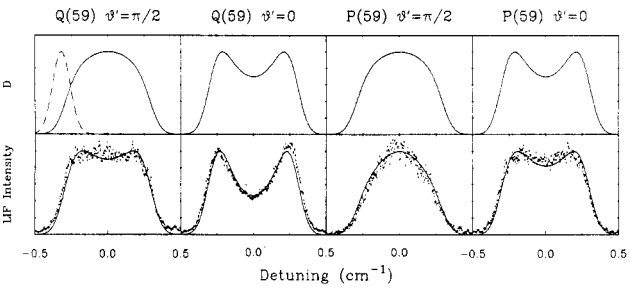

Figure 13. Experimental and calculated data for the Q(59) and P(59) lines of CO produced in the photodissociation of OCS and probed by laser-induced fluorescence on the $COA^1\Pi \leftarrow X^1\Sigma$ transition using circularly polarized light. The dissociation and LIF probe lasers were orthogonal. Fluorescence was detected without polarization selection at an angle of 45° to each laser beam. Upper row: Doppler profiles expected in the absence of v–J correlation (solid lines) calculated from eq 4; the Gaussian laser line width is shown in the dashed curve. Bottom row: Experimental profiles (dots) and profiles calculated for $\mathbf{v} \perp \mathbf{J}$ using eq 6 (solid curves). Along each row, the left panel is for the Q(59) line with the electric vector of the dissociating light $\hat{\mathbf{E}}$ aligned perpendicular to the propagation vector of the probe light Z ($\theta' = 90°$), the second panel is for the Q(59) line with $\hat{\mathbf{E}} \| \mathbf{Z}$ ($\theta' = 0°$), the third panel is for the P(59) line with $\hat{\mathbf{E}} \perp \mathbf{Z}$ ($\theta' = 90°$), and the last panel is for the P(59) line with $\hat{\mathbf{E}} \| \mathbf{Z}$ ($\theta' = 0°$). Calculations using either eq 4 or 6 are made with values of $\beta = 0.6$ for the recoil anisotropy, 0.14 cm^{-1} for the fwhm laser line width, and 1232 m s^{-1} for the velocity, as determined by energy and momentum conservation. The relationship between the angular variable χ and the detuning is $\Delta\nu = (\nu_0/c)v_0 \cos\chi$, where ν_0 is the center frequency and c is the speed of light. Reprinted with permission from ref 58. Copyright 1986 Royal Society of Chemistry.

By contrast, two groups have found that v and J are parallel in the photodissociation of H_2O_2.[50,51] Docker et al.[51] dissociated H_2O_2 at 248 nm and observed that the Doppler profiles of the OH $P_1(15)$ and $Q_1(15)$ lines were drastically different; the P_1 lines showed a substantial dip in the center of the profile, while the Q_1 lines did not. For the particular geometry employed in this experiment, the effect could be explained if there were a tendency for v and J to be parallel to one another. Such a tendency might arise if dissociation of H_2O_2 were accompanied by substantial torsional motion about the O–O bond.

Similar results were found by Gericke et al.[50] for H_2O_2 dissociation at 266 nm, for which a rather complete analysis was performed using the theory of Dixon,[52] described above. From analysis of the bipolar moments, these authors determined that the recoil anisotropy could be described by the conventionally defined anisotropy parameter $\beta = -0.71$, indicating that μ and v tend to be perpendicular. Although there was very little net alignment of J in the laboratory frame, a tendency was found for the rotational angular momentum vector to lie in a plane defined by v and μ with a somewhat larger projection along the v axis than along the μ axis. Such a situation might arise if, in addition to the torsional contribution to OH rotation, there were some contribution from the vibrational motion of the H_2O_2 parent.

VI. Other Vector Correlations

Several correlations involving vectors other than $\hat{\mathbf{E}}$, μ, v, and J have also been shown to be of importance in elucidating the dynamics of photodissociation. Perhaps the most closely related

(64) Balint-Kurti, G. G.; Shapiro, M. *Chem. Phys.* **1981**, *61*, 137.
(65) Balint-Kurti, G. G.; Shapiro, M. *Annu. Rev. Phys. Chem.* **1985**, *60*, 403.

is the observation of unequal populations among Λ doublets in open-shell fragments. In the high-J limit, population of the two Λ doublet levels can be viewed as two limiting cases of a correlation between **J** and a vector along the half-filled molecular orbital. One Λ doublet corresponds to the configuration in which the half-filled orbital lies in the plane of molecular rotation (perpendicular to **J**), while the other corresponds to the configuration when the half-filled orbital lies out of the plane (parallel to **J**). The half-filled orbital typically has a fixed angular relationship to the bond framework of the parent molecule in much the same way as does the recoil velocity. Thus, the correlation expressed by the Λ doublet populations is closely related to the **v**–**J** correlation. Neither depends on the laboratory frame of reference, and either provides information about the geometry of the transition state to dissociation. In practice, when the fragment possesses Λ doubling of rotational levels, it is often experimentally more easy to measure their relative populations than to measure the **v**–**J** correlation. But not all fragments have Λ doubling, whereas the **v**–**J** correlation can be measured in principle for any fragment.

That photodissociation can produce unequal populations of Λ doublet levels was first observed by Alberti and Douglas,[66] but the explanation for the effect was provided only later in an experiment by Quinton and Simons.[30] In both studies, NH_3 was dissociated in the vacuum-UV to yield H_2 + NH($c^1\Pi$). Resolved emission of rotationally excited states of the NH($c^1\Pi$) showed a preference for the half-occupied orbital of NH to lie perpendicular to the plane of fragment rotation. This preference is consistent with a model for the dissociation in which the change in NH_3 geometry from pyramidal to planar creates the torque which provides rotational excitation to the NH.

A more recent and very detailed study of this effect in the dissociation of H_2O has been presented by Andresen and coworkers.[39] A J-dependent Λ doublet inversion was observed for dissociation of H_2O prepared in low rotational levels by supersonic expansion, although no inversion was observed at room temperature. The J dependence of the Λ doublet inversion was found to be due to mixing between the two levels at low J. The absence of inversion at high initial temperatures was explained by the presence under these conditions of out-of-plane rotation in the parent compound, which couples with the OH rotation to mix the Λ doublets. The half-filled orbital of the OH was found to lie in a direction perpendicular to the plane of OH rotation, as expected for planar dissociation of the parent compound. The observations made by Andresen et al. provide strong evidence that the mechanism for the astronomical OH maser is a photochemical one.

(66) Alberti, F.; Douglas, A. E. *Chem. Phys.* **1978**, *34*, 399.

Several other vector correlations are currently under investigation, but as yet they are incompletely understood. For example, Nadler et al.[12] observed in the photodissociation of ICN that the spin-rotation levels of the CN fragment were unequally populated. This apparent anomaly has been addressed recently by Joswig, O'Halloran, Zare, and Child,[67] who find qualitative agreement between the data and a theory in which out-of-plane, spin-dependent forces cause the electron spin on the CN to have a preferred orientation with respect to rotation of the CN fragment. Another correlation currently under investigation is that between the parent rotation and the breaking bond in symmetric triatomic molecules.[68]

VII. Conclusions

The measurement of vector correlations in molecular photodissociation dynamics can provide important information both about the parent compound and about the mechanism by which it fragments. These correlations can be measured by monitoring the polarization properties and/or Doppler profiles of the fragments and can be understood on simple physical grounds. The $\hat{\mathbf{E}}$–μ–**v** and $\hat{\mathbf{E}}$–μ–**J** correlations allow one to determine the symmetry of the dissociative state, while the **v**–**J** and $\hat{\mathbf{E}}$–μ–(**v**–**J**) correlations provide information about the direction of repulsive forces at the moment of dissociation. For triatomic dissociations, a direct relationship using the theory of Balint-Kurti and Shapiro can be made between the correlated velocity and angular momentum distribution and the dissociative potential energy surfaces of the parent compound.[64,65] Vector correlations will certainly continue to play an important role in the elucidiation of photodissociation dynamics.

Acknowledgment. I thank several colleagues without whose help this work would not have been possible. Foremost among them are Prof. I. Burak and Dr G. E. Hall, who were instrumental both in developing the theory of **v**–**J** correlations and also in obtaining much of our experimental data in this area. Prof. J. W. Hepburn, Dr. G. Chawla, Dr. N. Sivakumar, Mr. C. Strauss, and Mr. G. McBane all contributed greatly to experiments concerning OCS and glyoxal. I am also grateful to Prof. R. N. Dixon for making his work available to me prior to its publication. Finally, I would like to acknowledge the support of the John Simon Guggenheim Foundation and of the National Science Foundation (Grant CHE-8314146) and to express my appreciation to the Fritz Haber Center for Molecular Dynamics and the Institute of Advanced Studies at the Hebrew University of Jerusalem for their hospitality during the preparation of this manuscript.

(67) Joswig, H.; O'Halloran, M. A.; Zare, R. N.; Child, M. S. *Discuss. Faraday Soc.*, in press.
(68) Valentini, J. J., private communication.